Characteristics of Corrosion Products of Friction-type High-Strength Bolted Joints of Steel Bridge: A Case Study

Gangnian Xu , Wenpeng Xu , Xu Dong * , Shengwei Fan , Xianggang Wang

Posted Date: 17 April 2023

doi: 10.20944/preprints202304.0431.v1

Keywords: steel bridge; connection node; friction type high-strength bolt; corrode; SEM; EDS; XRD

Article

Characteristics of Corrosion Products of Friction-type High-Strength Bolted Joints of Steel Bridge: A Case Study

Gangnian Xu [1], Wenpeng Xu [1], Xu Dong [1,*], Shengwei Fan [1] and Xianggang Wang [2]

[1] School of Transportation and Civil Engineering, Shandong Jiaotong University, Jinan 250357, China; 204144@sdjtu.edu.cn; xu19554107685@outlook.com ; 204129@sdjtu.edu.cn; 204014@sdjtu.edu.cn; wangxianggang@cncccg.com

[2] China National Chemical Communications Construction Group CO., LTD, Jinan250102, China; wangxianggang@cncccg.com

* Correspondence: 204129@sdjtu.edu.cn

Abstract: This paper analyzed the main diseases of the friction high-strength bolt (FHSB) joints in order to study the characteristics of the corrosion products of the joints in steel bridge and the influence factors. Seven representative FHSB connection pairs and eight steel plate samples were selected from the Dongying Shengli Yellow River Bridge, which has been in operation for 33 years. Then Scanning Electron Microscope (SEM), Energy Dispersive Spectroscopy (EDS) and X-Ray Diffraction (XRD) were used to analyze the microscopic morphology and chemical composition of the corroded surface of the samples. Finally, this paper discussed the relationship between the corroded sample surface and the environmental corrosion. The research results showed that construction quality problems, such as non-standard hole expansion, segmental slab joint dislocation and contact surface pollution, accelerated corrosion of the contact surface. With the increase of corrosion degree of joints, the contact surface of aluminum spraying layer gradually changed from a rugged and dense state to a smooth and porous powder state. With the corrosion of the steel plate substrate, the contact surface gradually changed from a fluffy stratified state to a surface bonding state. It was inferred that the friction coefficient of the FHSB connection node on the corroded aluminum sprayed contact surface first decreased and then increased. The corroded node samples detected not only a large number of S and Cl elements, but also the oxides of Mn, Si and other elements as well as FeS. It was speculated that node corrosion was also related to atmospheric (acid rain) and industrial dust and other corrosive environments. Almost all samples detected the component SiO2 of the Yellow River soil, as well as Mg, Ca, K, Na and other elements at the same time, which is basically consistent with the component elements of the Yellow River soil. Therefore, it was inferred that it was related to the inclusion of the Yellow River soil.

Keywords: steel bridge; connection node; friction type high-strength bolt; corrode; SEM; EDS; XRD

1. Introduction

The working mechanism of the FHSB is mainly to clamp the connecting plate through the strong clamping force generated by bolt fastening, and transfer the shear force perpendicular to the screw axis through the friction force generated by the indirect contact surface of the connecting plate. The FHSB is widely used in steel structure bridges, because it has advantages of high connection strength, simple and convenient construction, and it can directly bear dynamic and fatigue loads[1–3].

Compared with other parts of the steel bridge, FHSB connection nodes are more prone to corrosion and deterioration, which is mainly reflected in their own structural characteristics and the role of surrounding corrosive media[4–8].Because of the frequent gaps between the FHSB connectors of the steel bridge, water and gas containing corrosive ions are easy to invade the node components and cause corrosion. Due to the concealment of FHSB joint diseases and the complexity of removing the joint, the analysis of corroded joint components is mainly based on indoor test. Using the XRD, the SEM, electrochemical technology and alternate dry and wet corrosion test, many scholars have studied the corrosion behavior and rust formation mechanism of steel plate in different atmospheric

Preprints (www.preprints.org) | NOT PEER-REVIEWED | Posted: 17 April 2023 doi:10.20944/preprints202304.0431.v1

corrosive environments[9,10]. Air pollutants, PH value and wet time have great influence on the formation of steel surface protective layer[11,12]. For high-strength bolts, Daniel et al. studied the characteristics of corrosion products formed in the contact and exposed areas of bolts and nut fasteners[13]. Wen et al. studied the causes of fracture failure of high-strength bolts of steel bridges in subtropical humid climate, and the results showed that corrosive environment and stress accelerated the impact on fracture failure[14]. Compared with industrial atmospheric environment, high-strength bolts showed higher corrosion sensitivity in marine atmospheric environment, which led to bolt loosening and fatigue crack of bolt thread[15,16]. Therefore, the corrosive environment caused serious corrosion behavior to the raw materials of the steel bridge, which is one of the main factors affecting the performance degradation of the FHSB connection joints of steel structures[17–19]. In conclusion, due to different corrosive environments of the FHSB connection nodes of the steel bridge, their corrosion behaviors and corrosion products are also different, therefore, it is of great research value to study the characteristics of corrosion products of the nodes on the real bridge and influence factors in complex environmental corrosive conditions, such as wet, industrial and dust climates.

Therefore, this paper first analyzed the main diseases of the FHSB connection nodes of the Dongying Shengli Yellow River Bridge, which has been in operation for 33 years. Then after selecting seven representative FHSB connection sub-samples and eight steel plate samples, the SEM, the EDS and the XRD were used to analyze the microscopic morphology and chemical composition of corrosion products on the sample surface. Finally this paper discussed the relationship between the corroded sample surface and environmental corrosion in order to provide reference for scientific anti-corrosion protection measures for the nodes in aging steel bridges in the future.

2. Node diseases

The Shengli Yellow River Bridge is the first cable-stayed bridge with steel box girder and orthogonal special-shaped plates built in China. Located in Kenli County, Dongying City, the bridge was completed and opened to traffic in October 1987. With the main bridge span arranged at (60.5+136.5+288+136.5+60.5) m, the main beam has 57 steel box sections and 56 transverse joints in total, and its cross section is a separated double-sided rectangular box. Six orthotropic bridge decks are symmetrically arranged in the middle of the cross section, with two in upstream and downstream box girders respectively, and four between the box girders. The top and bottom plates are U-shaped closed ribbed orthotropic plates, most of which are 12 mm thick. Figure 1 is the schematic diagram of FHSB connection nodes for transverse joints. The transverse joint nodes of the whole bridge are connected by more than 110,000 sets of 10.9 M22 FHSB, and the diameter of bolt opening is 24.5 mm. The seam between the steel box sections is 6 mm wide, and the splice plate is 10 mm thick. The design value of the friction coefficient of the aluminum spraying contact surface is 0.45, and the longitudinal joint connection is field groove welding. The pavement is composed of epoxy resin coal tar anti-skid layer, 40 mm bottom layer and 30 mm surface layer rubber asphalt. Figure 2 is the schematic diagram of the components of the FHSB connection node.

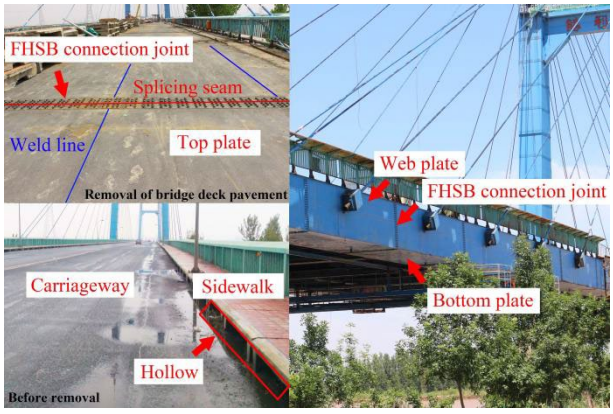

Figure 1. Schematic diagram of transverse joint FHSB connection node.

Preprints (www.preprints.org) | NOT PEER-REVIEWED | Posted: 17 April 2023 doi:10.20944/preprints202304.0431.v1

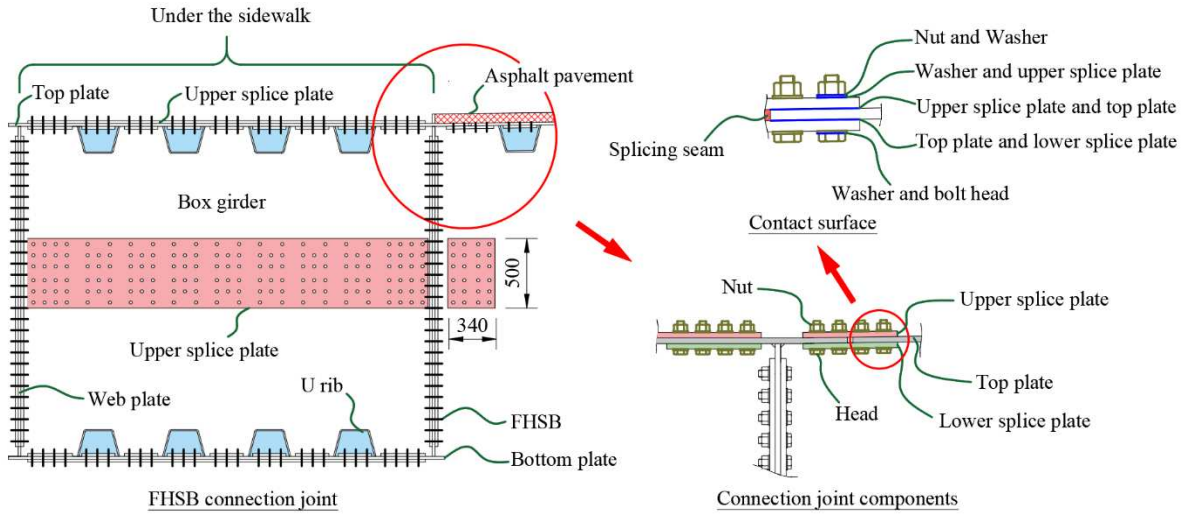

Figure 2. Schematic diagram of components of FHSB connection node.

Figure 3 shows some typical diseases of the transverse joint FHSB connection node. Due to exposure of the top plate of the box girder at the lower-part sidewalk and cracking of the pavement, the nodes were corroded by rain and corrosive gas all year round, resulting in serious corrosion of the nodes, with some nuts losing up to 65% thickness. In addition, the longitudinal ribs of the top and bottom plates at the FHSB nodes of the transverse joints had open butt welds, and the rigidity of the bridge deck was seriously weakened, resulting in different polishing degrees among the joint connecting components. The main diseases of FHSB connection nodes of transverse joints included coating peeling, corrosion of connection components, and polishing of section plate joints and bolt holes. Investigation and analysis showed that the number of bolt holes not expanded according to the specifications accounted for 9.62% of the total. Some gusset plate bolt holes were polished around and the polished shape was generally a circle with different areas, with an average 11 mm diameter. The number of polished bolt holes accounted for 15.22% of the total. Construction quality problems, such as nonstandard hole expansion, staggered slab joints and contact surface pollution, led to poor tightness of FHSB connection joint contact surface and accelerated corrosion of joint contact surface.

Preprints (www.preprints.org) | NOT PEER-REVIEWED | Posted: 17 April 2023 doi:10.20944/preprints202304.0431.v1

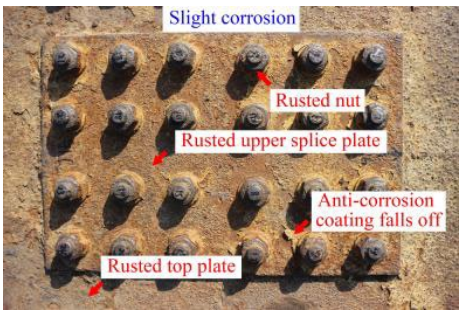

(a) The coating layer of the node in the traffic lane falls off

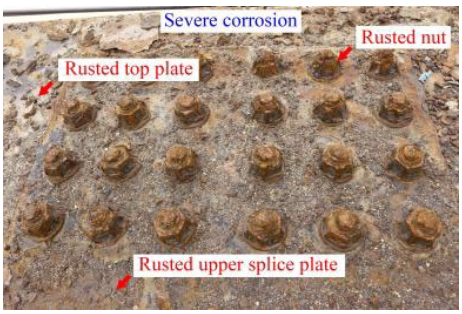

(b) Severely rusted nuts at the sidewalk

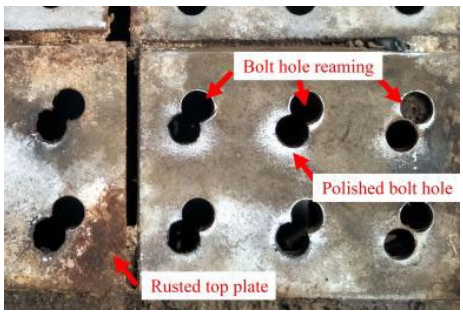

(c) Bolt hole reaming and peripheral polishing

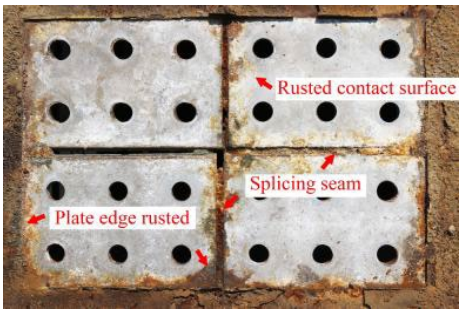

(d) Rusted edge of the plate joint and polished periphery of the bolt hole

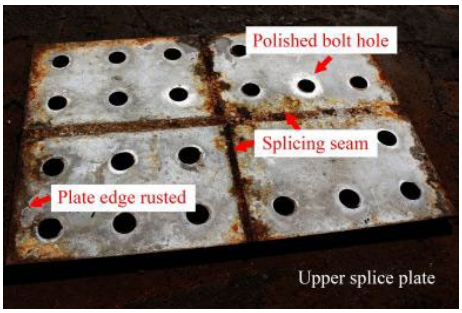

(e) Seriously rusted upper splice plate

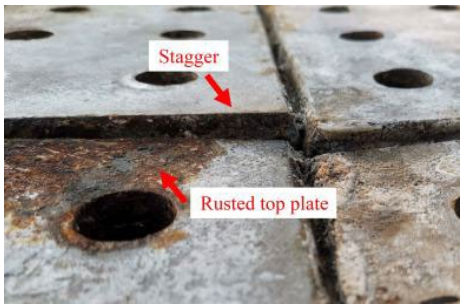

(f) Segmental slab seam staggering

Figure 3. Typical diseases of transverse joint FHSB connection nodes.

3. Analysis of node corrosion products

3.1. Samples of test pieces

In order to study the surface characteristics of the FHSB connection node assembly, fifteen representative samples at different positions of the node were selected. Table 1 describes the sample material, sampling location and surface corrosion degrees. A total of seven samples were selected from the surface of the high-strength bolt connection pair, with three (Head-1~Head-3) from the bolt head, two nuts (Nut-1 and Nut-2), and two gaskets (Washer-1 and Washer-2). Among these samples, three (Head-1,Nut-1 and Nut-2) were in direct contact with the atmosphere, two (Head-2 and Head-3) were in contact with the gasket, and two (Washer-1 and Washer-2) were in contact with the upper splice plate. A total of eight samples were selected from the surface of the connecting steel plate assembly, with two (Plate-1 and Plate-2) from the contact surface of the lower splice plate, five (Plate-3~Plate-7) from the contact surface of the upper splice plate, and one (Plate-8) from the contact surface of the roof. Among these samples, five (Plate-1,Plate-2 and Plate-4~Plate-6) were in contact with the roof, and three (Plate-3, Plate-7 and Plate-8) were in direct contact with the atmosphere. It should be particularly pointed out that six samples (Plate-1~Plate-6) were mainly used to study the characteristics of corrosion products of aluminum sprayed steel plate contact surface with different corrosion degrees. Sample selection position legend is shown in Figure 4.

Preprints (www.preprints.org) | NOT PEER-REVIEWED | Posted: 17 April 2023 doi:10.20944/preprints202304.0431.v1

Table 1. Description of sample material, sampling location and surface corrosion degrees[20–22].

Joint components	Specimen ID	Material	Selection position	Contact medium	Description of surface features
FHSB connection pair	Head-1	40B	Bolt head	Atmosphere	With the anti-corrosion coating falling off, the surface is slightly rusted and red.
	Head-2			Washer	No rust is found by naked eye, and local parts are polished and shiny.
	Head-3			Washer	No rust is found by naked eye, and local polishing is shiny, with obvious boundary.
	Nut-1	45	Nut	Atmosphere	The outer layer of the nut is severely rusted and reddish brown.
	Nut-2			Atmosphere	The inner layer of the nut is severely rusted and brown black.
	Washer-1		Washer	Upper splice plate	Slightly rusted, partially polished and shiny.
	Washer-2			Upper splice plate	No rust is found with naked eye, and there is obvious boundary.
Steel plate	Plate-1	16Mnq	Lower splice plate	Roof	No rust is found by naked eye, and the aluminum coating is shiny.
	Plate-2			Roof	The aluminum coating is slightly rusted and gray.
	Plate-3		Upper splice plate	Atmosphere	The aluminum spraying layer is severely rusted and reddish brown.
	Plate-4			Roof	The aluminum spraying layer is severely rusted and reddish brown.
	Plate-5			Roof	The aluminum coating is slightly rusted and gray.
	Plate-6			Roof	The aluminum spraying layer is severely rusted and has gray white powder.
	Plate-7			Atmosphere	With the anti-corrosion coating falling off, the surface is slightly rusted and red.
	Plate-8		Top plate	Atmosphere	Severely rusted, and brown black.

Preprints (www.preprints.org) | NOT PEER-REVIEWED | Posted: 17 April 2023 doi:10.20944/preprints202304.0431.v1

Figure 4. Sample selection position legend.

The instrument model used in this test is ZEISS SIGMA 500 field emission SEM made in Germany, which is used to observe the surface morphology of the sample, infer the corrosion products and surface morphology from the microscopic traces, and analyze the chemical composition of the substrate and corrosion layer by energy spectrum. The material structure of corrosion products was analyzed by German D8 ADVANCE A25 X-ray powder diffractometer. After being ground into fine powder of less than 200 mesh in an agate mortar, powdery substances were placed on the sample tank and their surface were flattened for testing. The measured surface of blocky substances was made flat and smooth as much as possible to ensure that the sample could be loaded into the φ 25 mm × 3 mm sample tank.

Preprints (www.preprints.org) | NOT PEER-REVIEWED | Posted: 17 April 2023 doi:10.20944/preprints202304.0431.v1

3.2. Micromorphology

Figure 5 shows the microscopic morphology of the sample surface. The SEM analysis results showed that the corrosion products on the surface of the bolt head (Head-1) are mostly scaly and loose. The corrosion products on the surface of Head-2 were mostly clastic, with loose structure, smooth local area and obvious boundary. Head-3 had compact structure, smooth local area and obvious boundary. The corrosion products of Nut-1 and Nut-2 were mainly needle shaped, and were also scaly and spiky. The micromorphology of gasket surface was basically similar to that of Head-2 and Head-3. The surface of Plate-1 aluminum spraying layer was uneven and in dense granular shape and was not rusted by naked eye. The surface of Plate-2 and Plate-5 aluminum spray coating was slightly rusted and dark gray, and its corrosion products were layered and cracked. Plate-6 aluminum spraying layer was seriously rusted, smooth and porous, and had white powder and loose surface structure. After the aluminum coating on the contact surface was completely corroded and the steel plate substrate gradually rusted, the corrosion products of Plate-3 and Plate-4 were reddish brown, with most of them being massive and spherical with obvious cracks. The surface protective layer of Plate-7 and Plate-8 in contact with the atmosphere basically fell off, with cluster corrosion products on the surface of Plate-7, and dense massive corrosion products on the surface of Plate-8, but there were many cracks and obvious delamination.

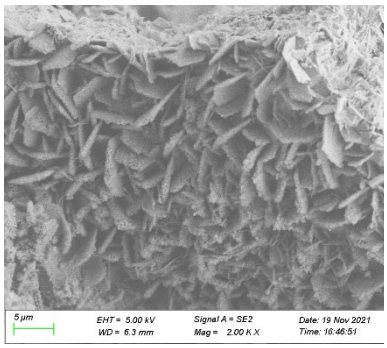

Head-1

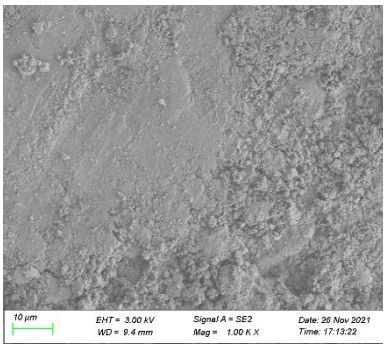

Head-2

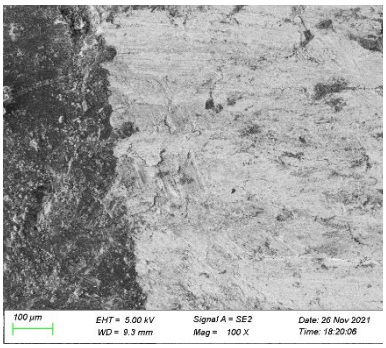

Head-3

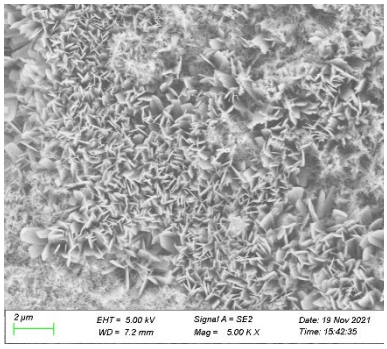

Nut-1

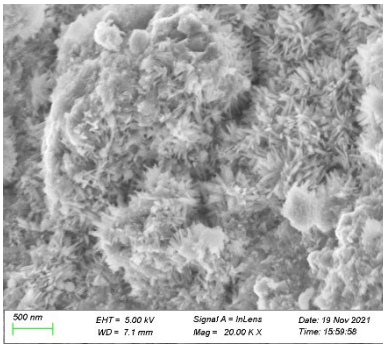

Nut-2

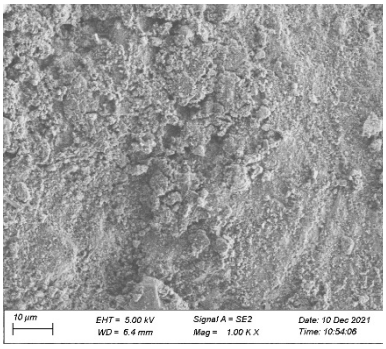

Washer-1

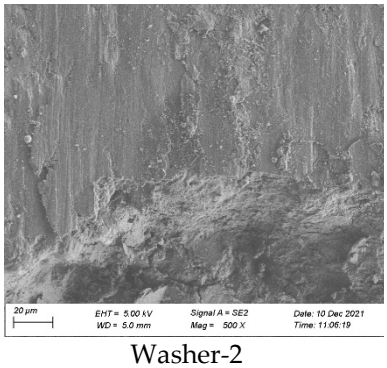

Washer-2

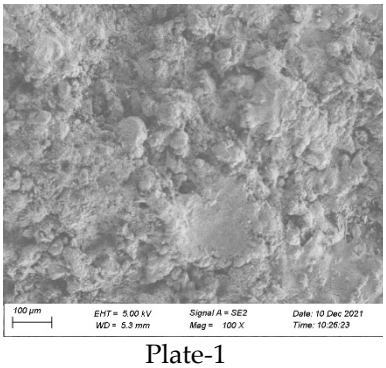

Plate-1

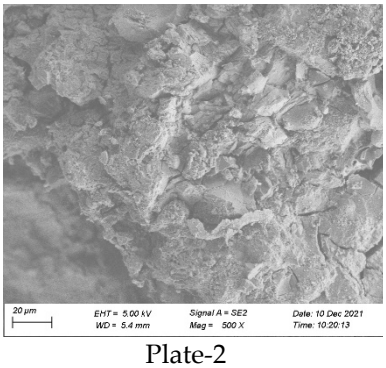

Plate-2

Preprints (www.preprints.org) | NOT PEER-REVIEWED | Posted: 17 April 2023 doi:10.20944/preprints202304.0431.v1

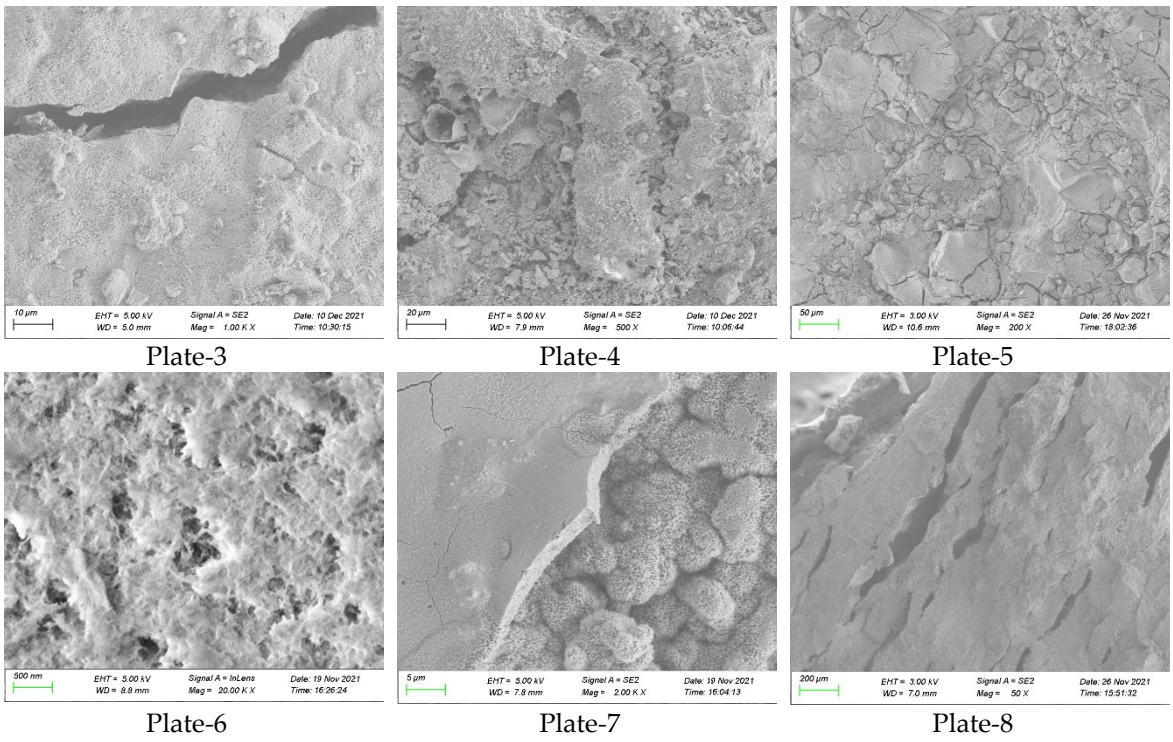

Figure 5. Micromorphology of sample surface.

In general, the micro-morphology of the corrosion products on the surface of each sample in contact with the atmosphere was relatively rich, which may be related to the complex corrosive environment of the connecting nodes. Debris accumulation occurred near the polished area formed by the contact surface, because sample polishing was mainly caused by the fretting and sliding of the connecting nodes. With the increase of corrosion degree, the contact surface of the aluminum spray coating on the steel plate gradually changed from an uneven and dense state to a smooth porous powder state. After the steel plate substrate gradually rusted, the corrosion product was fluffy and cracked red rust. With the lack of oxygen in the plate seam, the rust gradually turned from red to brown, and the surface was bonded. Therefore, the uneven "biting" state of the aluminum sprayed steel plate contact surface constantly changed. It was deduced that the friction coefficient of the contact surface decreased first and then increased. In addition, the polishing around the bolt hole changed the roughness and bonding state of the uneven contact surface, and also reduced the friction coefficient of the contact surface.

3.3. Chemical composition

Table 2 shows the specification values of the main elements in the sample matrix and the EDS results of corroded surface. The results showed that the elements mainly come from the elements of the sample itself and the corrosive ions in the environment. The surface material of the high-strength bolt connection pair sample is composed of main elements (Fe, O and C), and other small elements (Mn, S, Mg, Ti, Ca, Al, Si, P, Cl, Zn, K, Na, etc.). The surface material of the steel plate sample is composed of main elements (Al, Fe, O and C), and other small elements (Mn, S, Mg, Ti, Ca, Si, P, Cl, Zn, K, Na, etc.). Several elements (S, Mg, Ca, Si, Cl and Na) were detected on the sample surface of Plate-1~Plate-2 and Plate-4~Plate-6. Several elements (Mn, Mg, Ca, Al, Cl, K and Na) were detected on the surface of Plate-3, Plate-7 and Plate-8 samples in contact with the atmosphere.

According to the literature,The sample matrix contained a small amount of elements, such as C, Mn, S, Si and P[20–22]. Dongying is an industrial oil refining city in China, which produced a large amount of nitrogen oxides, sulfur dioxide and chloride ions, resulting in more acid rain weather in this area. A large amount of S and Cl elements were detected in the corrosion products of the sample. It was speculated that the sample corrosion maybe was related to atmospheric corrosion (acid rain).

 doi:10.20944/preprints202304.0431.v1

Test results showed that the solid suspended particles in the atmosphere around the Dongying Shengli Yellow River Bridge were mainly composed of Mg, Ca, Al, Si, K and Na, which are basically consistent with the elements of the Yellow River soil. Therefore, this paper speculated that Mg, Ca, Si, K and Na elements existing in the corrosion products of the sample maybe was related to the inclusion of Yellow River soil.

3.4. Phase Analysis

Table 2. Specification values of main elements in sample matrix and the EDS results of surface corrosion products[20–22].

Specimen	Fe	O	C	Mn	S	Mg	Ti	Ca	Al	Si	P	Cl	Zn	K	Na
Standard			0.37~0.44	0.60~0.90						0.20~0.40					
Head-1	52.79~93.69	3.33~38.84	1.70~9.43	0.41~0.75	0.13~0.55	0.36~0.72		0.16~0.34	0.08~1.10	0.20~1.05		0.11~0.28		0.24~0.36	1.11~2.37
Head-2	41.29~86.89	32.62~34.31	11.21~18.07	0.67~0.83			0.19~0.38	0.27~0.32	0.25~0.94	0.23~1.70	0.37~2.90		0.26~2.62		2.34~2.53
Head-3	48.62~64.35	10.40~32.18	8.14~22.56	0.45~0.58						0.28~1.30		0.25~0.34	0.94~1.95		
Standard			0.42~0.50	0.50~0.80	≤0.04					0.17~0.37	≤0.04				
Nut-1	54.96~60.08	36.40~37.27	2.97~5.71	0.55~1.80				0.15~0.27		0.17~0.24		0.14~0.37		0.38~0.51	0.85~2.54
Nut-2	57.11~63.11	32.79~37.14	3.69~5.01	0.41~0.74		0.14~0.32						0.13~0.21			
Standard			0.42~0.50	0.50~0.80	≤0.04					0.17~0.37	≤0.04				
Washer-1	6.01~26.69	14.23~28.51	53.50~54.51		0.23~1.38	0.51~0.86		0.87~2.61	0.53~2.37	0.57~1.87	0.42~1.75	0.39~1.99	0.11~1.46	0.30~0.40	0.46~1.28
Washer-2	14.89~25.26	17.53~24.53	44.43~56.46		0.39~0.79	0.26~0.54		0.28~2.32	3.01~4.56	0.76~2.29				0.16~0.53	
Standard			≤0.20	1.20~1.35	≤0.004					1.20~1.35	≤0.015				
Plate-1		3.51~3.99	3.93~5.86			0.18~0.64			88.09~90.05			0.35~0.84			
Plate-2	6.52~15.62	7.92~21.21	1.64~4.30			0.44~0.65	0.08~0.13	1.25~2.00	11.31~42.51	2.76~3.61					0.73~1.12
Plate-3	42.42~88.59	7.19~46.19	2.87~6.27			0.24~0.31		0.32~1.43	0.37~1.75			0.98~5.13		0.83~1.29	
Plate-4	25.16~56.62	23.88~35.11	4.64~5.63	0.61~2.34	0.42~0.94	0.41~0.84		1.32~2.41	1.20~3.24	0.58~1.17	0.78~1.77	0.78~1.37	0.53~1.95	0.99~4.99	0.56~2.03
Plate-5	0.85~4.95	34.38~54.53	4.71~10.83		0.16~0.61	0.29~0.79	0.15~0.26	0.42~3.45	5.10~39.09	0.34~2.02	0.12~0.16	1.24~3.65		0.28~1.16	0.13~4.10
Plate-6		54.33~62.83	4.61~7.49		0.57~0.81			1.88~2.35	26.74~36.72			0.26~1.42			
Plate-7	67.81~87.48	7.94~26.31	1.36~3.48	0.43~1.40		0.18~0.22		0.17~1.27		0.35~1.64		0.35~2.36		0.67~1.62	
Plate-8	61.56~80.96	16.52~32.86	1.82~4.34	0.60~1.73					0.10~0.82	0.15~0.21					1.42~3.05

Preprints (www.preprints.org) | NOT PEER-REVIEWED | Posted: 17 April 2023 doi:10.20944/preprints202304.0431.v1

Figure 6 shows the XRD pattern of corrosion products on the sample surface. Analysis results showed that the corrosion products of bolt head, nut, gasket and outer surface of steel plate were mainly Fe and Si oxides. In addition, the corrosion products of Head-1 contained FeS, that of Nut-1 and Nut-2 contained MnO_2 and FeOOH, and that of Plate-7 and Plate-8 contained Mn_2O_3 and FeOOH. The corrosion products of steel plate contact surface samples were mainly Al and Fe oxides, most of which were Al_2O_3, Fe_2O_3 and Fe_3O_4.

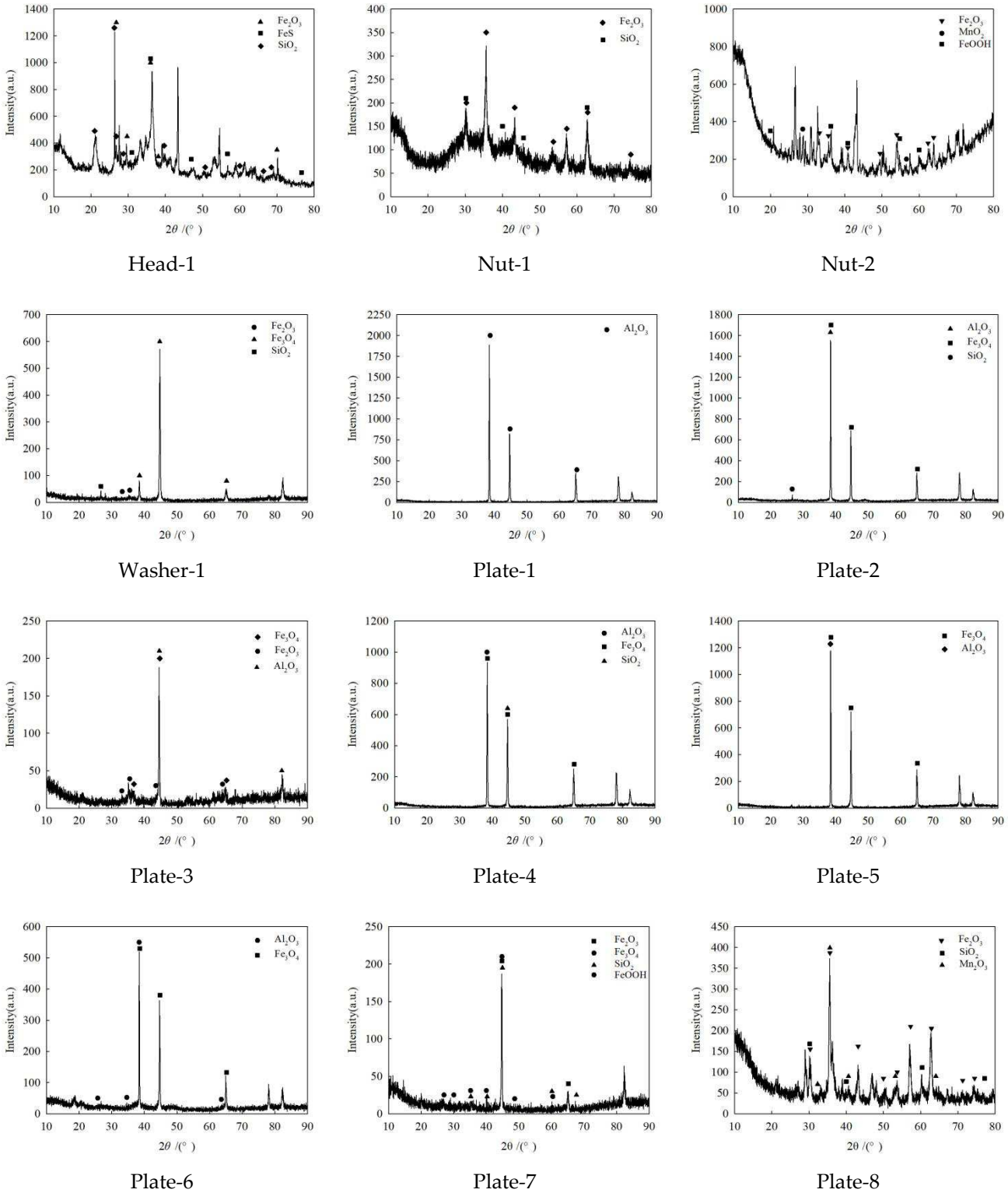

Figure 6. The XRD pattern of sample.

 doi:10.20944/preprints202304.0431.v1

Table 3 shows the XRD results of the main corrosion products on the sample surface. It can be seen from the table that the corrosion products of most steel plate contact surface samples are Al_2O_3, and Fe_2O_3 and Fe_3O_4 are also detected in the severely corroded samples. When corrosive ions, oxygen, water and dust invaded the joint, the aluminum layer on the joint contact surface was sprayed for oxidation first, and the white powder gradually formed after the block fell off. The corrosion product was mainly Al_2O_3. With the corrosion of steel plate substrate, the surface corrosion products were mainly Fe_2O_3 and Fe_3O_4. The XRD phase analysis results showed that the sample also contained oxides of Mn, Si and other elements as well as FeS. It was speculated that the node corrosion was also related to atmospheric (acid rain) and industrial dust and other corrosive environments. In addition, the XRD pattern of silty yellow soil showed that SiO_2, Al_2O_3 and Fe_2O_3 were the main oxide components amd almost all samples detected the component SiO_2 of the Yellow River soil. Because the silty yellow river soil was easily adsorbed on the node components after being blown up, the wet yellow river environment all year round may accelerate the node corrosion.

Table 3. The XRD results of main corrosion products on sample surface.

Specimen	Contact medium	Products
Head	Atmosphere	Fe_2O_3, FeS, SiO_2
Nut	Atmosphere	Fe_2O_3, MnO_2, FeOOH, SiO_2
Washer	Interface	Fe_2O_3, Fe_3O_4, SiO_2
Plate	Interface	Al_2O_3, Fe_3O_4, SiO_2
	Atmosphere	Al_2O_3, Fe_2O_3, Fe_3O_4, Mn_2O_3, FeOOH, SiO_2

Conclusions

In order to study the characteristics of corrosion products of FHSB connection joints and the influence factors, this paper first analyzed the main diseases of the joints in Dongying Shengli Yellow River Bridge. After seven representative FHSB connection sub-samples and eight steel plate samples were selected, then the SEM, the EDS and the XRD were used to analyze the microscopic morphology and chemical composition of the corrosion products on the sample surface. Finally, this paper discussed the relationship between the corrosion products on the sample surface and the environmental corrosion. The main conclusions were as follows:

(1) Construction quality problems, such as nonstandard hole expansion, stagger of segmental plate joints and pollution of contact surface, made the contact surface of the FHSB connection node not tight enough and accelerated the corrosion of the contact surface.

(2) With the increase of corrosion degree of joints, the contact surface of aluminum spraying layer gradually changed from a rugged and dense state to a smooth and porous powder state. With the corrosion of the steel plate substrate, the surface of the contact surface gradually changed from a fluffy stratified state to a surface bonding state. It was inferred that the friction coefficient of the FHSB joint on the corroded aluminum sprayed contact surface first decreased and then increased.

(3) The corrosion products of the node samples not only detected a large number of S and Cl elements, but also the oxides of Mn, Si and other elements as well as FeS. It was speculated that the node corrosion was also related to atmospheric (acid rain) and industrial dust and other corrosive environments.

(4) Almost all samples detected the component SiO_2 of the Yellow River soil, as well as Mg, Ca, K, Na and other elements. Because this is basically consistent with the component elements of the Yellow River soil, it was inferred that it was related to the inclusion of the Yellow River soil.

Author Contributions: Conceptualization, X.G.N., X.W.P. and D.X.; methodology, X.G.N. and X.W.P.; validation, X.G.N., X.W.P., D.X., F.S.W. and W.X.G.; formal analysis, D.X.; investigation, X.G.N.; resources, X.G.N.; writing—original draft preparation, X.G.N. and X.W.P.; writing—review and editing, D.X. and F.S.W.; visualization, X.G.N.; supervision, X.G.N.; project administration, X.G.N.; funding acquisition, X.G.N. and W.X.G. All authors have read and agreed to the published version of the manuscript.

Funding: This work is supported by (a) the National Natural Science Foundation of China (No. 51578325), (b) the Youth Foundation of Shandong Natural Science Foundation of China (No. ZR2021QE279) and (c) the Open Project of Key Laboratory of Transportation Industry (Beijing) for Old Bridge Detection and Reinforcement Technology (No. 2021-JQKFKT-3).

Institutional Review Board Statement: Not applicable.

Informed Consent Statement: Not applicable.

Data Availability Statement: Not applicable.

Conflicts of Interest: The authors declare no conflict of interest.

References

1. Shah, J. K.; Braga, H. B. F.; Mukherjee, A.; Uy, B. Ultrasonic monitoring of corroding bolted joints. *Eng. Fail. Anal.* **2019**, *102*, 7-19.
2. Zhang, C. Q.; Su, M. Z.; Zhu, C. H.; Wang, M. M. Bearing performance of high-strength bolted corrugated steel longitudinal seams. *J. Constr. Steel Res.* **2022**, *198*, 107538.
3. Xu, G. N.; Wang, Y. Z.; Du, Y. F.; Zhao, W. S.; Wang, L. Y. Static Strength of Friction-Type High-Strength Bolted T-Stub Connections under Shear and Compression. *Appl. Sci.* **2020**, *10*, 3600.
4. Li, M.; Yao, L. B.; Zhang, S. S.; Wang, D. P.; He, Z. Q.; Sun, G. H. Study on bolt head corrosion influence on the clamping force loss of high strength bolt. *Eng. Fail. Anal.* **2021**, *129*, 105660.
5. Kim, T. S.; Lee, H. S.; Yoo, J. H.; Tae, S. H.; Oh, S. H.; Lim, Y. C.; Lee, S. B. Slip Coefficient in High-Strength Bolt Joints Coated with Corrosion-Resistant Zn/Al Metal Spray Method. *Mater. Manuf. Process.* **2011**, *26*, 14-21.
6. Jiang, C.; Xiong, W.; Cai, C. S.; Zhu, Y. J.; Liu, Z. X. Experimental study on the shear behavior of friction connections with corrosion damage. *J. Constr. Steel Res.* **2022**, *197*, 107449.
7. Wang, H. L.; Tang, F. J.; Qin, S. F.; Tu, K. Y.; Guo, J. Q. Corrosion-Induced Mechanical Degradation of High-Strength Bolted Steel Connection. *J. Mater. Civil. Eng.* **2020**, *32*, 04020203.
8. Kim, I.-T.; Lee, J. M.; Huh, J. W.; Ahn, J.-H. Tensile behaviors of friction bolt connection with bolt head corrosion damage: Experimental research B. *Eng. Fail. Anal.* **2016**, *59*, 526-543.
9. Zhang, Y. W.; Guo, T. M.; Song, Z. T.; Nan, X. L.; Xu, X. J.; Dong, Z. L. Corrosion Behavior of Q345q Steel with Oxide Scale in Simulated Typical Atmospheric Environment in Northwest China. *J. Mater. Res.* **2019**, *33*, 749-762.
10. Li, N.; Zhang, W. F.; Xu, H.; Cai, Y. K.; Yan, X. J. Corrosion Behavior and Mechanical Properties of 30CrMnSiA High-Strength Steel under an Indoor Accelerated Harsh Marine Atmospheric Environment. *Materials.* **2022**, *15*, 629.
11. Křivý, V.; Kubzová, M.; Konečný, P.; Kreislová, K. Corrosion Processes on Weathering Steel Bridges Influenced by Deposition of De-Icing Salts. *Materials.* **2019**, *12*, 1089.
12. Honarvar Nazari, M.; Allahkaram, S. R.; Kermani, M. B. The effects of temperature and pH on the characteristics of corrosion product in CO2 corrosion of grade X70 steel. *Mater. Des.* **2010**, *31*, 3559-3563.
13. Felix, D. E.; Li, C.; Wang, C. G.; Dong, J. H.; Ime, U. I.; Chukwuemeka, O. P.; Zhang, D. J.; Zhong, W. A.; Zhong, S. Insights into the characteristics of corrosion products formed on the contact and exposed regions of C1045 steel bolt and nut fasteners exposed to aqueous chloride environments. *J. Mater. Sci. Technol.* **2023**, *135*, 250-264.
14. Wen, J.; Chen, L.; Duan, X.; Yang, J.; Liu, Q. C.; Liu, L. Fracture Failure Performance of 35VB Steel High-Strength Bolts Used in Subtropical Humid Climate. *J. Mater. Civil. Eng.* **2021**, *33*, 04021359.
15. Yang, X. K.; Zhang, L. W.; Zhang, S. Y.; Zhou, K.; Li, M.; He, Q. Y.; Wang, J. C.; Wu, S.; Yang, H. M. Atmospheric Corrosion Behaviour and Degradation of High-Strength Bolt in Marine and Industrial Atmosphere Environments. *Int. J. Electrochem. Sci.* **2021**, *16*, 151015.
16. Lachowicz Maciej, B.; Lachowicz Marzena, M. Influence of Corrosion on Fatigue of the Fastening Bolts. *Materials.* **2021**, *14*, 1485.
17. Jiang, C.; Xiong, W.; Cai, C. S.; Zhou, X. Y.; Zhu, Y. J. Corrosion effects on the fatigue performance of high-strength bolted friction connections. *Int. J. Fatigue.* **2023**, *168*, 107392.
18. Kong, Z. Y.; Yang, F.; Jin, Y.; Hong, S. Z.; Wang, X. Q.; Vu, Q.-V.; Truong, V.-H.; Yu, B.; Kim, S.-E. Experimental study on bearing capacity of corroded high-strength bolt connections under shear force. *Constr. Build. Mater.* **2021**, *309*, 125117.

19. Goran, V.; Goran, V.; Spiro, I. Tensile strength behaviour of steel plates with corrosion-induced geometrical deteriorations. *Ships. Offshore. Struc.* **2022**, *17*, 2611-2619.
20. National Standards of the People's Republic of China. *Grade and general technical conditions of high-quality carbon structural steel*; GB 699-1965; Ministry of Metallurgical Industry: Beijing, China, **1965**.
21. Trade Standards of the People's Republic of China. *Structural steel for bridge*; YB (T) 10-1981; Ministry of Metallurgical Industry: Beijing, China, **1981**.
22. Trade Standards of the People's Republic of China. *Technical Conditions for Alloy Structural Steel*; YB6-1971; Ministry of Metallurgical Industry: Beijing, China, **1971**.